JOURNAL OF SOLID STATE CHEMISTRY 37, 219–227 (1981)

The Crystal Structure of a New Mixed Oxide of Iron and Vanadium, $(Fe,V)_{18}O_{35}$

I. E. GREY,* M. ANNE, A. COLLOMB, J. MULLER, AND M. MAREZIO

Laboratoire de Cristallographie, C.N.R.S. 166 X, 38042 Grenoble, Cédex, France

Received June 3, 1980; in final form August 26, 1980

Single crystals of a new compound, $Fe_{6.5}V_{11.5}O_{35}$, have been prepared by hydrothermal synthesis at 650°C and 2 kbar. The compound has triclinic symmetry, $P\bar{1}$, $Z = 1$, with unit cell dimensions $a = 10.209(3)$, $b = 9.387(3)$, $c = 6.564(2)$ Å, $\alpha = 100.52(5)$, $\beta = 94.35(5)$, $\gamma = 98.85(4)°$. Its structure was determined using direct methods and refined to an R-value of 0.053 ($wR = 0.038$) for 5654 observed reflections ($F > 3\sigma(F)$) whose intensities were measured on a Philips PW1100 diffractometer using Ag$K\alpha$ radiation. The structure is based on a cubic close-packed framework of anions in which cations are ordered into tetrahedral (V^{5+}), square pyramidal (V^{4+}), and octahedral (Fe^{3+}, $V^{4+,3+}$) sites. The structure comprises zig-zag chains of eight edge-shared octahedra (α-PbO_2-like) which are cross linked via corner-sharing with tetrahedra and square pyramids, and via edge-sharing with square pyramids and octahedra. Bond length–bond strength considerations were used to establish the cation valence-state assignments at the different sites, giving a unit cell composition $Fe^{3+}_{6.5}V^{3+}_{1.5}V^{4+}_{4}V^{5+}_{6}O_{35}$.

1. Introduction

The synthesis and structural characterization of a new phase with composition $FeV_2O_6 \cdot H_{0.5}$ has recently been reported (*1*). Its structure is closely related to that of diaspore, from which it may be derived by the ordered displacement of every third octahedrally coordinated metal in the double-chains of edge-shared octahedra, into an adjacent tetrahedral site in the channels between the double-chains. This phase was formed in a hydrothermal experiment at 650°C and 2 kbar, aimed at synthesizing the mixed oxide, $Fe^{3+}V^{4+}V^{5+}O_6$ (*2*). However, the subsequent structure analysis showed that some anion sites were partially occupied by hydroxyl ions and that its composition was actually $Fe^{3+}V^{3+}_{0.5}V^{4+}_{0.5}V^{5+}O_{5.5}(OH)_{0.5}$. The hydrothermal experiments carried out at 650°C yielded, in addition to crystals of the above phase, some crystals of a second phase with quite different morphology. An electron probe analysis gave a composition quite close to FeV_2O_6. In the belief that this phase was the mixed oxide $Fe^{3+}V^{4+}V^{5+}O_6$, we carried out a crystal-structure determination, the results of which are reported here.

2. Experimental

2.1. Preparation and characterization

A 1:1 mixture of $FeVO_4$ and VO_2 was reacted for 5 days at 650°C and 2 kbar in

* Permanent address: CSIRO Division of Mineral Chemistry, P.O. Box 124, Port Melbourne, Victoria, Australia.

0022-4596/81/050219-09$02.00/0

Copyright © 1981 by Academic Press, Inc.
All rights of reproduction in any form reserved.

hydrochloric acid solution. The initial pH of the solution was close to 1 but at the completion of the reaction it had increased to 2. A heterogeneous product was obtained comprising mainly small black platelets of $FeV_2O_6H_{0.5}$, together with some black needles of iron-doped VO_2, and a few columar crystals of the new phase. A powder pattern obtained from finely ground crystals showed some similarities to that for $FeV_2O_6 \cdot H_{0.5}$ in the distribution of the strong reflections but showed many extra strong and medium intensity peaks. The powder pattern was indexed with the aid of precession photographs which showed that the symmetry was triclinic. A refinement of 2θ values for 28 powder lines led to the unit cell parameters, $a = 10.209(3)$, $b = 9.387(3)$, $c = 6.564(2)$ Å, $\alpha = 100.52(5)$, $\beta = 94.35(4)$, $\gamma = 98.85(4)°$. An electron microprobe analysis on crystals of the compound, using iron and vanadium metals as standards, gave Fe, 24.71 and V, 39.44 weight percent, corresponding to a V/Fe ratio of 1.75 (cf. 2.00 in the original reaction mixture).

2.2. Single crystal studies

The crystals grown by hydrothermal synthesis were columnar, with approximately square cross-section, 0.1 to 0.2 mm wide, and 0.5 to 1 mm long. For the intensity data collection, a fragment was cut from one of the crystals, measuring 0.13 × 0.16 × 0.19 mm. Initially, precession photographs were taken to confirm it was a single crystal. It was then remounted along its long dimension on a Philips PW1100 4-circle diffractometer. Intensities were collected with graphite monochromated Ag$K\alpha$ radiation. An ω-scan, 3–30° in θ was used with a variable scan width given by $\Delta\theta = (1.40 + 0.15 \tan\theta)$ and a speed of 0.02° sec^{-1}. Two background measurements, each for half the scan time, were made for each scan, one at the lower and one at the upper limit. There were 7711 reflections measured in the hemisphere out to $\theta = 30°$. These were reduced to 7269 independent reflections of which 5654 had $F > 3\sigma(F)$ and were used in the refinement. An absorption correction was not applied, $\mu = 43.9$ cm^{-1}.

Scattering factor curves for V, Fe, and O neutral atoms are those of Doyle and Turner (*3*). Anomalous dispersion corrections were applied for all atoms (*4*). The X-ray system of programs was used for all aspects of the structure determination and refinement.

3. Structure Determination and Refinement

The structure was solved in space group $P\bar{1}$ by direct methods, using the MULTAN program. The set of generators included 11 known phases from the sigma 1 relationships, 3 origin determining reflections, and 4 unknowns, leading to 16 possible solutions. Initially an E-map was calculated using phases for the unknowns corresponding to the highest combined FOM (figure of merit). The positions of 8 metal atoms were located and refined, and 18 oxygen atoms were located in a subsequent difference Fourier map. However, we were unable to refine the model below an R-value of 0.17 and the temperature factors displayed a wide range of positive and negative values. At this stage it was decided to abandon the model and look at the E-map corresponding to the next highest FOM, 2.78 (cf. 2.90 for the first map). The value of psi zero was lowest for this set of signs and the corresponding calculated E-map led to the correct model for the structure. The greater reliability of the psi-zero value relative to the combined FOM is well established for space groups having no or few translational symmetry elements.

The positions of 9 metal atoms were located from the E-map. Refinement of their coordinates gave an R-value of 0.36. A difference-Fourier revealed the positions of

TABLE I

$Fe_{6.5}V_{11.5}O_{35}$: FRACTIONAL ATOMIC COORDINATES AND TEMPERATURE FACTOR COEFFICIENTS[a]

Atom	x	y	z	U_{11}	U_{22}	U_{33}	U_{12}	U_{13}	U_{23}
M(1)	0.38198(5)	0.00505(5)	0.34189(8)	0.65(2)	0.66(2)	0.64(2)	0.11(2)	0.02(2)	0.11(2)
M(2)	0.41738(5)	0.30556(6)	0.20229(9)	1.13(2)	0.62(2)	0.58(2)	0.06(2)	0.00(2)	0.16(2)
M(3)	0.70031(6)	0.00284(6)	0.16619(9)	0.60(2)	0.65(2)	0.56(2)	0.11(2)	0.09(2)	0.06(2)
M(4)	0.50781(6)	0.68489(6)	0.29032(9)	0.63(2)	0.61(2)	0.55(2)	0.20(2)	0.10(2)	0.10(2)
M(5)	0.10557(6)	0.30164(6)	0.38373(9)	0.69(2)	0.59(2)	0.48(2)	0.13(2)	0.10(2)	0.05(2)
M(6)	0.01298(7)	0.93745(7)	0.25177(14)	0.91(3)	1.06(3)	5.41(5)	0.25(2)	−0.00(3)	−0.82(3)
M(7)	0.81805(5)	0.64649(6)	0.09079(8)	0.74(2)	0.82(2)	0.72(2)	0.11(2)	0.05(2)	0.18(2)
M(8)	0.78192(7)	0.37963(6)	0.27240(9)	1.41(3)	0.44(2)	0.50(2)	0.14(2)	0.13(2)	0.06(2)
M(9)	0.18551(6)	0.71694(6)	0.21951(9)	0.67(2)	0.63(2)	0.61(2)	0.15(2)	0.11(2)	0.14(2)
O(1)	0.0000	0.0000	0.0000	1.64(18)	1.29(16)	1.08(16)	0.14(13)	0.16(14)	0.57(14)
O(2)	0.4315(3)	0.5232(3)	0.3132(4)	1.26(12)	0.94(10)	1.34(12)	0.24(9)	0.29(9)	0.10(9)
O(3)	0.0024(3)	0.7301(3)	0.1513(4)	0.68(11)	0.75(10)	1.07(11)	0.09(8)	0.05(8)	−0.12(8)
O(4)	0.6064(3)	0.3418(3)	0.2416(5)	2.05(14)	1.56(12)	1.93(13)	0.92(14)	0.90(11)	0.64(10)
O(5)	0.9879(3)	0.3871(3)	0.3109(4)	1.02(12)	1.04(11)	1.07(11)	0.37(9)	0.08(9)	0.13(9)
O(6)	0.8084(3)	0.5950(3)	0.3788(4)	1.15(12)	0.74(10)	0.61(10)	0.10(8)	0.08(8)	−0.08(8)
O(7)	0.4046(3)	0.2252(3)	0.4674(4)	1.20(12)	0.73(10)	1.04(11)	0.36(9)	0.06(9)	0.24(8)
O(8)	0.1927(3)	0.6512(3)	0.4332(4)	1.44(13)	1.19(11)	0.92(11)	0.20(10)	0.15(9)	0.27(9)
O(9)	0.3860(3)	0.0807(3)	0.0776(4)	1.15(12)	0.88(10)	0.92(11)	0.07(9)	0.07(9)	0.20(9)
O(10)	0.3840(3)	0.7852(3)	0.2255(4)	0.82(11)	0.65(10)	0.97(11)	0.07(8)	0.03(9)	0.03(8)
O(11)	0.1923(3)	0.5625(3)	0.9919(4)	1.02(11)	0.70(10)	0.78(10)	0.19(8)	0.13(8)	0.14(8)
O(12)	0.7808(3)	0.1679(3)	0.1476(4)	1.14(12)	0.76(10)	1.50(12)	0.02(9)	0.31(9)	0.02(9)
O(13)	0.1974(2)	0.9274(3)	0.3016(4)	0.59(10)	0.74(10)	1.30(11)	0.02(8)	−0.05(8)	0.02(8)
O(14)	0.0327(3)	0.1318(3)	0.4300(4)	1.16(12)	0.84(10)	0.87(11)	0.10(9)	0.16(9)	0.02(8)
O(15)	0.8128(3)	0.8962(3)	0.2263(4)	0.91(12)	1.25(11)	1.25(12)	0.28(9)	0.00(9)	0.49(9)
O(16)	0.6127(3)	0.6631(3)	0.0936(4)	1.03(12)	1.26(12)	0.64(10)	0.22(9)	0.16(9)	0.23(9)
O(17)	0.5875(3)	0.0171(3)	0.3575(4)	0.81(11)	1.14(11)	0.78(10)	0.10(9)	0.09(9)	0.28(9)
O(18)	0.2113(3)	0.2951(3)	0.1843(4)	0.94(12)	1.31(11)	0.64(10)	0.43(9)	0.02(9)	0.18(8)

[a] Thermal parameters $\times 10^2$ for all atoms. esd's given in parentheses.

18 oxygen atoms and their inclusion in the structure factor calculation led to an R-value of 0.15. Full matrix refinement of all positional and isotropic temperature factors reduced the R-value to 0.08. At this stage a difference-Fourier revealed peaks about 0.25 Å on either side of the metal atom site M(6) along [001]. Attempts were made to replace M(6) by a "split-pair" of atoms but refinement of the coordinates always led to a merging of the two atoms, with consequent reappearance of the subsidiary side peaks in the difference Fourier. A more satisfactory approach was the conversion to anisotropic temperature factors for all atoms. With composite Fe/V scattering curves for all metal atom sites, estimated from bond-length–bond-strength calculations (see below), refinement of all positional parameters and anisotropic temperature factors resulted in convergence at $R = 0.053$, $wR = 0.038$ for 5654 reflections with $F > 3\sigma(F)$. Before the final refinement, the intensity data were corrected for an isotropic extinction parameter, $g = 0.61 \times 10^{-6}$. This value was determined from a plot of $|F_c|/|F_o|$ versus I_c and not further refined. The final parameters are given in Table I. Calculated bond lengths and angles are given in Table II.*

* The list of observed and calculated structure factors may be obtained by request to the authors.

TABLE II

$Fe_{6.5}V_{11.5}O_{35}$: INTERATOMIC DISTANCES (Å) AND ANGLES (°)

	Distance	O–M–O angle		Distance	O–M–O angle		Distance	O–M–O angle
M(3) tetrahedron (V^{5+})			M(4) tetrahedron (V^{5+})			M(5) tetrahedron (V^{5+})		
M(3)–O(9)	1.715(2)		M(4)–O(2)	1.632(3)		M(5)–O(5)	1.633(3)	
O(12)	1.666(3)		O(7)	1.761(2)		O(6)	1.763(2)	
O(15)	1.706(3)		O(10)	1.761(3)		O(14)	1.740(3)	
O(17)	1.768(3)		O(16)	1.744(3)		O(18)	1.757(3)	
O(9)–O(12)	2.768(3)	108.2(1)	O(2)–O(10)	2.731(4)	107.1(1)	O(5)–O(18)	2.696(4)	105.3(1)
O(12)–O(15)	2.754(4)	109.5(1)	O(2)–O(16)	2.751(4)	109.1(1)	O(5)–O(14)	2.744(4)	108.8(1)
O(9)–O(15)	2.798(4)	108.0(1)	O(2)–O(7)	2.758(3)	108.7(1)	O(6)–O(14)	2.827(3)	107.6(1)
O(12)–O(17)	2.838(4)	111.4(1)	O(7)–O(10)	2.865(4)	108.9(1)	O(5)–O(6)	2.879(4)	108.6(1)
O(15)–O(17)	2.842(4)	109.8(1)	O(10)–O(16)	2.881(4)	110.6(1)	O(6)–O(18)	2.897(4)	110.8(1)
O(9)–O(17)	2.882(4)	109.9(1)	O(7)–O(16)	2.911(4)	112.3(1)	O(14)–O(18)	2.958(4)	115.5(1)
M(1) octahedron (Fe^{3+},V^{3+})			M(2) octahedron (Fe^{3+},V^{3+})			M(6) octahedron (Fe^{3+},V^{4+})		
M(1)–O(7)	2.050(2)		M(2)–O(2)	2.019(3)		M(6)–O(1)	1.855(1)	
O(9)	1.994(3)		O(4)	1.898(3)		O(3)	1.918(3)	
O(10)	2.069(2)		O(7)	2.024(3)		O(13)	1.908(3)	
O(13)	1.890(3)		O(9)	2.083(3)		O(14)	1.951(2)	
O(17)	2.077(3)		O(16)	2.024(3)		O(14)′	2.356(3)	
O(17)′	2.027(3)		O(18)	2.086(3)		O(15)	2.006(3)	
O(10)–O(13)	2.519(4)	78.9(1)	O(7)–O(9)	2.646(4)	80.2(1)	O(3)–O(13)	2.501(3)	81.6(1)
O(7)–O(10)	2.646(4)	81.7(1)	O(2)–O(4)	2.664(5)	85.7(1)	O(1)–O(15)	2.680(3)	87.80(9)
O(17)–O(17)′	2.710(4)	82.6(1)	O(16)–O(18)	2.692(4)	81.8(1)	O(3)–O(15)	2.685(4)	86.3(1)
O(10)–O(17)	2.726(3)	82.2(1)	O(2)–O(18)	2.814(3)	86.6(1)	O(14)′–O(15)	2.730(4)	77.0(1)
O(7)–O(17)′	2.738(4)	84.4(1)	O(4)–O(7)	2.828(4)	92.3(1)	O(14)–O(14)′	2.796(4)	80.4(1)
O(9)–O(17)	2.860(4)	89.2(1)	O(9)–O(16)	2.830(4)	87.1(1)	O(13)–O(14)	2.801(4)	93.1(1)
O(9)–O(13)	2.882(4)	95.7(1)	O(7)–O(18)	2.841(4)	87.5(1)	O(1)–O(14)	2.839(2)	96.46(9)
O(13)–O(17)′	2.925(4)	96.5(1)	O(2)–O(16)	2.875(3)	90.6(1)	O(1)–O(3)	2.885(3)	99.75(9)
O(7)–O(17)	2.941(4)	90.9(1)	O(9)–O(18)	2.918(4)	88.9(1)	O(3)–O(14)′	2.889(4)	84.4(1)
O(10)–O(17)′	2.978(4)	93.3(1)	O(4)–O(16)	3.007(4)	100.1(1)	O(14)–O(15)	2.937(3)	95.8(1)
O(9)–O(10)	3.102(4)	99.5(1)	O(4)–O(9)	3.029(4)	99.0(1)	O(1)–O(13)	2.962(3)	103.85(9)
O(7)–O(13)	3.188(3)	107.9(1)	O(2)–O(7)	3.124(4)	101.2(1)	O(13)–O(14)′	3.083(4)	92.0(1)

M(7) octahedron (Fe^{3+},V^{3+})			M(8) octahedron (Fe^{3+},V^{4+})			M(9) square pyramid (V^{4+})		
M(7)–O(3)	1.906(3)		M(8)–O(4)	1.758(3)		M(9)–O(3)	1.919(3)	
O(6)	2.042(3)		O(5)	2.087(3)		O(8)	1.634(3)	
O(11)	1.922(2)		O(6)	1.985(2)		O(10)	2.023(3)	
O(15)	2.362(3)		O(12)	2.005(3)		O(13)	1.933(3)	
O(16)	2.126(3)		O(8)	2.007(3)		O(11)	1.894(2)	
O(18)	1.995(3)		O(11)	1.938(3)				
O(6)–O(11)	2.610(3)	82.3(1)	O(6)–O(11)	2.610(3)	83.4(1)	O(3)–O(13)	2.501(3)	81.0(1)
O(3)–O(15)	2.685(4)	77.1(1)	O(5)–O(8)	2.612(4)	79.3(1)	O(10)–O(13)	2.519(4)	79.1(1)
O(16)–O(18)	2.692(4)	81.5(1)	O(4)–O(12)	2.629(5)	88.4(1)	O(8)–O(10)	2.742(4)	96.6(1)
O(15)–O(16)	2.714(3)	74.2(1)	O(5)–O(12)	2.709(3)	82.9(1)	O(10)–O(11)	2.764(3)	89.7(1)
O(3)–O(6)	2.850(4)	92.4(1)	O(5)–O(11)	2.763(4)	86.6(1)	O(3)–O(11)	2.828(4)	95.8(1)
O(6)–O(16)	2.860(4)	86.6(1)	O(4)–O(11)	2.790(4)	97.9(1)	O(3)–O(8)	2.857(4)	106.8(1)
O(15)–O(18)	2.923(3)	83.8(1)	O(6)–O(8)	2.811(4)	89.5(1)	O(8)–O(11)	2.864(4)	108.3(1)
O(3)–O(18)	2.929(4)	97.3(1)	O(4)–O(8)	2.827(4)	97.1(1)	O(8)–O(13)	2.870(4)	106.8(1)
O(11)–O(18)	3.032(4)	101.4(1)	O(11)–O(12)	2.828(4)	91.6(1)	O(11)–O(13)	3.640(3)	144.1(1)
O(3)–O(11)	3.078(3)	107.1(1)	O(4)–O(6)	2.851(4)	99.0(1)	O(3)–O(10)	3.831(4)	152.9(1)
O(11)–O(16)	3.131(4)	101.2(1)	O(5)–O(6)	2.879(4)	89.9(1)			
O(6)–O(15)	3.163(4)	91.5(1)	O(8)–O(12)	2.923(4)	93.5(1)			

Shared-edge M–M distances

M(1)–M(1)	3.083(1)	M(1)–M(2)	3.099(1)	M(1)–M(9)	3.042(1)	M(2)–M(7)	3.103(1)	M(6)–M(7)	3.078(1)
M(6)–M(9)	2.909(1)	M(7)–M(8)	2.950(1)						

4. Description of the Structure

From the structure analysis, the total number of metal atoms and oxygens in the unit cell are 18 and 35, respectively (see Table I). Together with the V/Fe ratio of 1.75 determined from the microprobe analysis, this leads to a unit cell composition of $Fe_{6.5}V_{11.5}O_{35}$ for the compound. Its structure is based on a cubic close packing of anions. The axial vectors for the c.c.p. anion subcell are parallel to [100]*, [032], and [0$\bar{1}$4]. The sequence of polyhedral layers perpendicular to [100]* is illustrated in Fig. 1. Each layer comprises pairs of edge-shared octahedra which are further connected by corner sharing either directly as for M(6), or via square pyramids, M(9), and tetrahedra, M(3), M(4), and M(5). The site M(9) derives from an octahedral interstice in the close-packed oxygen framework, by a displacement of the cation away from O(12) toward the vertice O(8). This results in a very long M(9)–O(12) bond of 2.838(3) Å and the coordination to M(9) is best described as square pyramidal. The tetrahedrally coordinated metals are located about 1 Å above and below the layer containing the 5- and 6-coordinated metals in Fig. 1. Interlayer articulation of the octahedral pairs M(7)–M(8) and M(1)–M(2) occurs by edge-sharing to produce zig-zag strings of 8 edge-shared octahedra directed approximately along [$\bar{2}$21]. This is seen most clearly if the structure is viewed perpendicular to the close-packed layers, which are parallel to ($\bar{2}$12), as illustrated in Fig. 2. The unit cell outline show in Fig. 2 is simply related to the original cell by $a' = -a + c$, $b' = a + c$, $c' = 2b - c$ and b', c' lie in the layers. The chains of 8 edge-shared octahedra are not interconnected either directly or indirectly within the close-packed layers. However, a comparison of Figs. 1 and 2 shows that extensive interlayer coupling occurs, via corner-sharing with the tetrahedra about M(3), M(4), and M(5), by edge- and corner-sharing with the square-pyramid about M(9) and by edge-sharing with the octahedral dimer about M(6).

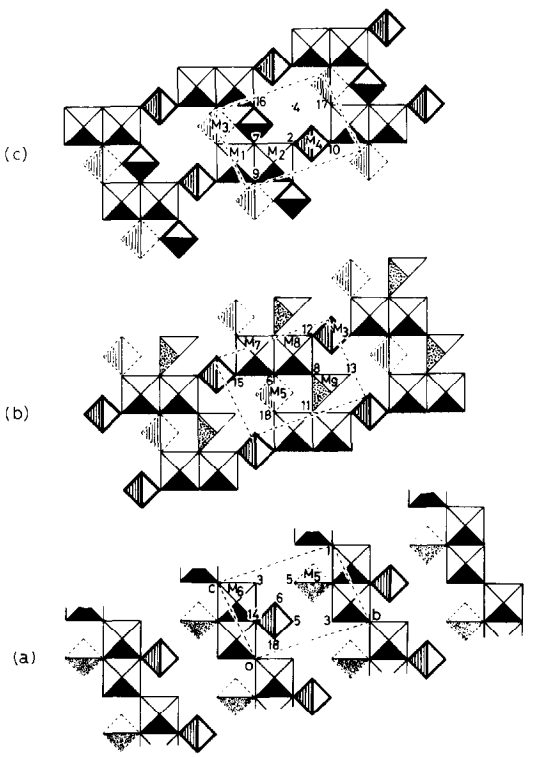

FIG. 1. (100) polyhedral layers in $Fe_{6.5}V_{11.5}O_{35}$ centred at $x = 0$ (a); $x = 0.2$ (b); $x = 0.4$ (c). The metals in the tetrahedra outlined in heavy lines and dashed lines lie ~1 Å above and below the layers, respectively. The intersection of the unit cell outline with each layer is shown by dashed lines. Individual numbers refer to oxygens (see Table I). Numbers prefixed with an M refer to metals.

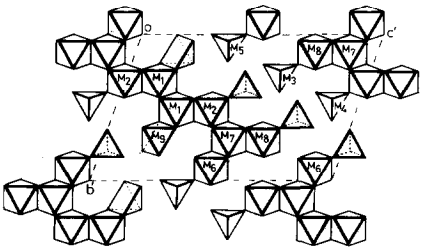

FIG. 2. Polyhedral representation of the structure of $Fe_{6.5}V_{11.5}O_{35}$ as viewed perpendicular to the close-packed oxygen layers.

5. Valence State Calculation

5.1. Cations

In Table III are listed the valences calculated for each cation using the empirical bond strength–bond length parameters for M–O bonds from Brown and Wu (5). It is clear that the tetrahedrally coordinated cations M(3), M(4), and M(5) are V^{5+} and the 5-coordinated cation M(9) is V^{4+}. The cations M(6) and M(8) have valences close to 3.5 and 3.67, respectively, which were considered to result from mixing of Fe^{3+} and V^{4+} in the ratios 1/1 and 1/2, respectively. The remaining three cations, M(1), M(2), and M(7), have valences close to 3 and are considered to be occupied by a mixture of Fe^{3+} and V^{3+}. The relative amounts of the two cations were made the same in the three sites and were calculated to be consistent with the known total vanadium and iron contents. The resulting unit cell composition is $Fe^{3+}_{6.5}V^{3+}_{1.2}V^{4+}_{4.3}V^{5+}_{6}O_{35}$. The formula so derived is not balanced, there being a deficiency of 0.3e per unit cell. Assuming the imbalance to be taken up in the V^{3+}/V^{4+} ratio (in the octahedral sites), the corresponding balanced formula is $Fe^{3+}_{6.5}V^{3+}_{1.5}V^{4+}_{4}V^{5+}_{6}O_{35}$. The imbalance may also be partly due to the presence of some Fe^{2+}, e.g., in site M(7), see Table III.

From Table I it is noted that the cation sites M(6) and M(8), which contain a mixture of Fe^{3+} and V^{4+}, have associated large anisotropic temperature factors. M(6) with equal occupancy by Fe^{3+} and V^{4+}, has an r.m.s. displacement parallel to c^* of 0.23 Å, whereas along a^* and b^* the values are less than half this figure, at 0.10 Å. The c^* direction is approximately along the line O(14)–M(6)–O(1) and thus it is probable that a local ordering of V^{4+} and Fe^{3+} occurs in the site M(6) so that when V^{4+} occupies the site it is displaced ~0.2 Å from the mean position toward O(1) to achieve square-pyramidal coordination with M(6)–O(1) ≃ 1.65 Å (as for site M(9) which contains only

TABLE III

CALCULATION OF CATION AND ANION VALENCES IN $Fe_{6.5}V_{11.5}O_{35}$, USING PARAMETERS FROM BROWN AND WU (5)

Cations			Anions				Anions		
Site	Cation valence	Cations at site	Site	Coordinating cations	Anion valence	Site	Coordinating valence	Anion valence
M(1)	3.00	1.6 Fe^{3+} + 0.4 V^{3+}	O(1)	M(6)(×2)	1.53	O(10)	M(1) + M(4) + M(9)	2.01
M(2)	2.96	1.6 Fe^{3+} + 0.4 V^{3+}	O(2)	M(2) + M(4)	2.09	O(11)	M(7) + M(8) + M(9)	1.97
M(3)	4.92	$2V^{5+}$	O(3)	M(6) + M(7) + M(9)	2.00	O(12)	M(3) + M(8)	1.97
M(4)	4.84	$2V^{5+}$	O(4)	M(2) + M(8)	1.73	O(13)	M(1) + M(6) + M(9)	2.01
M(5)	4.95	$2V^{5+}$	O(5)	M(5) + M(8)	2.02	O(14)	M(5) + M(6)(×2)	1.95
M(6)	3.44	Fe^{3+} + V^{4+}	O(6)	M(5) + M(7) + M(8)	2.07	O(15)	M(3) + M(6) + M(7)	1.99
M(7)	2.86	1.6 Fe^{3+} + 0.4 V^{3+}	O(7)	M(1) + M(2) + M(4)	2.02	O(16)	M(2) + M(4) + M(8)	2.01
M(8)	3.66	0.7 Fe^{3+} + 1.3 V^{4+}	O(8)	M(8) + M(9)	2.03	O(17)	M(1)(×2) + M(3)	1.96
M(9)	4.01	$2V^{4+}$	O(9)	M(1) + M(2) + M(3)	2.05	O(18)	M(2) + M(5) + M(7)	2.03

V^{4+}). On the other hand, when the site is occupied by Fe^{3+}, it takes up a position approximately 0.2 Å closer to O(14), thus tending to equalize the distances M(6)–O(1) and M(6)–O(14) to give octahedral coordination. A similar argument applies to site M(8), containing $\frac{1}{3}Fe^{3+} + \frac{2}{3}V^{4+}$. In this case the largest r.m.s. displacement, 0.12 Å, is along a^* (cf. 0.07 Å along b^* and c^*), i.e., along the line O(5)–M(8)–O(4). When the site is occupied by V^{4+}, the cation is displaced ~0.1 Å toward O(4) to give M(8)–O(4) = 1.65 Å with an accompanying movement of O(5) away from M(8). When Fe^{3+} occupies the site it will be displaced ~0.1 Å toward O(5), thus tending to equalize M(8)–O(4) and M(8)–O(5) to give octahedral coordination. Further support for this "local-ordering" model derives from its ability to explain the apparent severe undersaturation of oxygens O(1) and O(4) as will be discussed below.

5.2. *Anions*

The valences calculated for each of the anions O(1)–O(18) are given in Table III. With the exception of O(1) and O(4), they differ by no more than 5% from the expected value of 2.00. Both O(1) and O(4) are severely undersaturated with valences of 1.53 and 1.73, respectively. It is tempting to use these results as evidence for partial occupancy of the anion sites by hydroxyl ions, particularly as hydroxyls were identified in the associated phase formed in the hydrothermal synthesis, $FeV_2O_6 \cdot H_{0.5}$. However, about 1.0 OH^- (per 35 anions) is needed to explain the above results and this would require a concomitant reduction in the cation valences which would be inconsistent with the results given in Table III. Alternatively, there would need to be vacancies in some of the cation sites; again this was not evident from the structure refinement. An alternative explanation for the low results is that we have not correctly represented the valence contributions from the ordered V^{4+} and Fe^{3+} in sites M(6) and M(8) in the calculation of the valences of O(1) and O(4) given in Table III. If, instead of using the mean M(6)–O(1) and M(8)–O(4) distances, we consider the individual distances for V^{4+} and Fe^{3+} we calculate valence sums for O(1) and O(4) very close to 2. For example, allowing a displacement of 0.23 Å of V^{4+} toward O(1) and Fe^{3+} away from O(1), we have V^{4+}–O(1) = 1.625 and Fe^{3+}–O(1) = 2.085 Å and the valence of O(1) is given as:

$$\begin{aligned} O(1) = 2 \times [&0.5s(V^{4+} - O(1)) \\ &+ 0.5s(Fe^{3+} - O(1))] \\ &= 1.56 + 0.41 = 1.97. \end{aligned}$$

Similarly, if we consider a displacement of 0.12 Å of V^{4+} and Fe^{3+} in site M(8), toward and away from O(4), respectively, then the valence at

$$\begin{aligned} O(4) = &s(M(2) - O(4)) \\ &+ [\tfrac{1}{3}s(Fe^{3+} - O(4) + \tfrac{2}{3}s(V^{4+}) - O(4))] \\ &= 0.69 + 0.25 + 1.03 = 1.97. \end{aligned}$$

The proposed ordering will affect also the calculation of the charge at the other anions bonded to M(6) and M(8) but in these cases the contributions are considerably weaker and the corresponding changes much smaller. Although the ordering of V^{4+} and Fe^{3+} in the M(6) and M(8) sites appears to give an adequate explanation for the apparent undersaturation at the anion sites O(1) and O(4), we cannot exclude the possibility of some hydroxyl ions at these sites. In all probability, both explanations apply partially.

6. Discussion

The compound with formula $Fe_{6.5}V_{11.5}O_{35}$ is unusual in that three separate valence states of vanadium coexist in the same phase. Of course, the valence states were

not determined directly and some doubt must exist concerning individual assignments of minor components. However, the assignments of V^{5+} to the tetrahedral sites M(3), M(4), M(5) and V^{4+} to the square pyramidal site M(9) are unambiguous and the remaining assignments are consistent with both overall and individual site charge requirements as well as the chemical composition, and relatively small departures from the assignments given in Table III result in obvious discrepancies. Although V^{3+} is oxidized by V^{5+} in solution, it appears that in a stable crystalline phase such as the iron vanadium oxide studied here where these ions occupy separate, distinct crystallographic sites, their coexistence is made possible by site-energy stabilization. A similar situation occurs in $FeV_2O_6 \cdot H_{0.5}$ (*1*), in which the distribution of valence states over the three independent sites is close to $(V^{5+})^{tet}(V^{3+}_{0.5}Fe^{3+}_{0.5})^{oct}(V^{4+}_{0.5}Fe^{3+}_{0.5})^{oct}O_6H_{0.5}$, i.e., V^{5+} and V^{3+} occur in the same compound, but in different sites with tetrahedral and octahedral coordination, respectively. A partial disproportionation of V^{4+} into V^{3+} and V^{5+} has also been reported to occur in the triclinic T structure of Al-doped VO_2. In this case all three valence-states of vanadium occur in octahedral sites. It is interesting to compare the two iron vanadium oxides $FeV_2O_6 \cdot H_{0.5}$ and $Fe_{6.5}V_{11.4}O_{35}$. Although both compounds were prepared under identical conditions and have very similar formulae, close to FeV_2O_6, and similar distributions of Fe^{3+}, V^{3+} and Fe^{3+}, V^{4+} in octahedral and V^{5+} in tetrahedral sites and the same 2:1 ratio of octahedral (+ square pyramidal) to tetrahedral sites, the two structures have little in common. Whereas the anion framework in $Fe_{6.5}V_{11.5}O_{35}$ forms a cubic close-packed array, that in $FeV_2O_6 \cdot H_{0.5}$ is strongly deformed from hexagonal close-packing. It may formally be derived from an ideal hexagonal close-packed array by a 20° rotation about *c* of two-octahedra-wide (010) slabs. Rotation of alternate blocks in opposite senses leads to an angle of 141° between the double chains of octahedra and creates tetrahedral sites in the channels between the chains (see Fig. 3 in Ref. *1*).

Both structures contain similar structure-building polyhedral clusters, i.e., edge-shared dimers, linked into chains by further edge sharing and cross-lined by corner sharing with tetrahedra, but the method of chain formation and cross-linking is different. For $Fe_{6.5}V_{11.5}O_{35}$, this is illustrated in Figs. 1 and 2 and described above. In the case of $FeV_2O_6 \cdot H_{0.5}$, the edge-sharing between dimers leads to crank-shaft-like infinite chains rather than 8-membered α-PbO_2-like zig-zag chains, and both individuals of the dimers share corners with a common tetrahedron (see Fig. 2 in Ref. *1*). The subtleties of multiple-valence stabilization and polyhedral articulation variations between 4-, 5-, and 6-coordinated sites in these compounds suggests that a rich variety of as yet undiscovered structures may be prepared by hydrothermal synthesis in the $FeVO_4$–VO_2–V_2O_3 system.

References

1. J. MULLER, J. C. JOUBERT, AND M. MAREZIO, *J. Solid State Chem.* **27**, 367 (1979).
2. A. BURDESE, *Ann. Chim. (Roma)* **47**, 817 (1957).
3. P. A. DOYLE AND P. S. TURNER, *Acta Crystallogr.* **A24** 390 (1968).
4. D. T. CROMER AND D. LIBERMAN, *J. Chem. Phys.* **53**, 1891 (1970).
5. I. D. BROWN AND K. K. WU, *Acta Crystallogr.* **B32** 1957 (1976).
6. J. MULLER, Ph.D. Thesis, Grenoble University (1977).
7. M. GHEDIRA, H. VINCENT, M. MAREZIO, AND J. C. LAUNAY, *J. Solid State Chem.* **22**, 423 (1977).